ARTICLE

doi:10.1038/nature24483

A Jurassic gliding euharamiyidan mammal with an ear of five auditory bones

Gang Han[1,2], Fangyuan Mao[3], Shundong Bi[4], Yuanqing Wang[3] & Jin Meng[5]

Gliding is a distinctive locomotion type that has been identified in only three mammal species from the Mesozoic era. Here we describe another Jurassic glider that belongs to the euharamiyidan mammals and shows hair details on its gliding membrane that are highly similar to those of extant gliding mammals. This species possesses a five-boned auditory apparatus consisting of the stapes, incus, malleus, ectotympanic and surangular, representing, to our knowledge, the earliest known definitive mammalian middle ear. The surangular has not been previously identified in any mammalian middle ear, and the morphology of each auditory bone differs from those of known mammals and their kin. We conclude that gliding locomotion was probably common in euharamiyidans, which lends support to idea that there was a major adaptive radiation of mammals in the mid-Jurassic period. The acquisition of the auditory bones in euharamiyidans was related to the formation of the dentary–squamosal jaw joint, which allows a posterior chewing movement, and must have evolved independently from the middle ear structures of monotremes and therian mammals.

Mammalia Linnaeus, 1758
Allotheria Marsh, 1880
Euharamiyida Bi, Wang, Guan, Sheng & Meng, 2014
Arboroharamiyidae Zheng, Bi, Wang & Meng, 2013
Arboroharamiya allinhopsoni sp. nov.

Etymology. The specific name is in honour of E. F. Allin and J. A. Hopson for their contribution to the study of mammalian middle ear evolution.

Types. The holotype (HG-M017) is a nearly complete skeleton with craniodental structures and fur impressions preserved. The paratype (HG-M018) is also a skeleton with well-preserved impressions of fur and gliding membrane, but its skull was broken (Fig. 1; Extended Data Figs 2, 3; Supplementary Information).

Locality and age. The specimens are from the Tiaojishan Formation in the same pit at the locality of Nanshimen village, Gangou Township, Qinglong County, Hebei Province, China. The age of the strata is interpreted as 164–159 million years, roughly correlative with the Oxfordian (Extended Data Fig. 1 and Supplementary Information).

Diagnosis. Dental formula I^1-C^0-P^2-M^2/I_1-C_0-P_1-M_2 (I, incisor; C, canine; P, premolar; M, molar; superscript, upper teeth; subscript, lower teeth) (Extended Data Fig. 4). Similar to *Arboroharamiya jenkinsi*[1] but differing from other euharamiyidans[2] in having a hypertrophic mesiolingual cusp (a1) on p4, P4 being transversely the widest upper tooth, and having a strong posterior process on the stapes (unknown in other species). Differs from *A. jenkinsi* in being smaller in body size (Extended Data Table 1) and having upper incisors without 'fluting', molars with fewer cusps and ridges in the basin, A1 more distally extended than B1 on upper molars, and the stapes proportionally shorter. Further differs from *Xianshou* in having one pair of upper incisors that are smaller than the enlarged upper ones of *Xianshou* (upper incisors known only in *Xianshou linglong*) and in each incisor having a main mesial cusp and several distal cuspules, cusp a1 of p4 being more developed, and having molars with more cusps. Further differs from *Shenshou* in having enlarged cusp a1 on lower cheek teeth and more cusps on molars, and the promontorium bearing the groove for the stapedial artery. Differs from *Haramiyavia*, *Thomasia*, and *Megaconus* in having only two upper and lower molars, basined upper premolars with enamel flutings, and larger a1 on the lower molars and A1 on the upper molars. Differs from eleutherodontids in having only two longitudinal rows of cusps and less extended cusp A1 on upper molars and more robust a1 on p4 and lower molars. Further differs from *Megaconus* in having basined cheek teeth instead of a trench-like longitudinal valley on molars, and a gracile skeleton for arboreal life. Differs from multituberculates, particularly the Mesozoic ones, in having two upper and one lower premolars and cusp a1 of m1 occluding in the valley of M1. Differences from *Maiopatagium*[3] and *Vilevolodon*[4] are given in Supplementary Information.

Description

The description focuses on the middle ear and gliding features (see Supplementary Information for additional description). The promontorium that houses the cochlea is almond-shaped and bulges ventrally (Fig. 2; Extended Data Fig. 5), similar to those of therians. On its posterior portion a transverse groove is interpreted as for the stapedial artery that passed laterally through the stapedial foramen of the stapes in life. The fenestra vestibuli is slightly tilted to face ventrolaterally and is separated by a narrow crista interfenestralis from the perilymphatic foramen; the latter is notched at the dorsomedial rim, as in multituberculates[5]. The fossa for the stapedius muscle is posterior to the fenestra vestibuli and posterolaterally bounded by the paroccipital process. Computed laminography reveals an elongate and curved cochlear canal, similar to that of multituberculates[5,6] (Fig. 2b).

The left auditory bones are preserved nearly in their original position, with the stapes articulating the incus and the other bones being slightly displaced anteriorly. The lower jaws are in an occlusal position and the auditory bones are fully separated from the dentary. The stapes has its footplate in the fenestra vestibuli, indicating that the footplate is slightly smaller than the fenestra vestibuli and was probably connected to the rim of the fenestra vestibuli by the annular ligament in life. The stapes is similar to that of *A. jenkinsi*[7]. It measures 1.2 mm

[1]Paleontology Center, Bohai University, Jinzhou, Liaoning Province, 121013, China. [2]Hainan Tropical Ocean University, Sanya, Hainan Province 572022, China. [3]Key Laboratory of Evolutionary Systematics of Vertebrates, Institute of Vertebrate Paleontology and Paleoanthropology, Chinese Academy of Sciences, PO Box 643, Beijing 100044, China. [4]Department of Biology, Indiana University of Pennsylvania, Indiana, Pennsylvania 15705, USA. [5]Division of Paleontology, American Museum of Natural History, New York, New York 10024, USA.

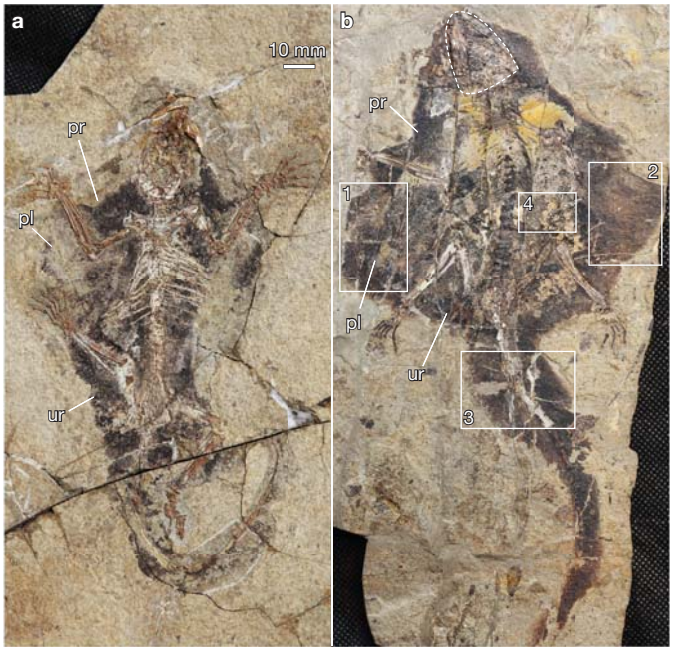

Figure 1 | Type specimens of *A. allinhopsoni*. **a**, Holotype (HG-M017-B), which shows a ventral view of limbs and impressions of body fur and gliding membrane. **b**, Paratype (HG-M018-A), which shows a ventral view of the skeleton and impressions of the gliding membrane and fur. The damaged but reconstructed skull was outlined to caution against misunderstanding of skull morphology. pl, plagiopatagium, the primary gliding membrane that extends between the forelimbs and hind limbs; pr, propatagium, the membrane between the neck and forelimbs; ur, uropatagium, the membrane between the hind legs and the tail. Boxes 1–4 in **b** correspond to **a**–**d** in Fig. 3. See Extended Data for additional morphologies. Scale bar applies to **a** and **b**.

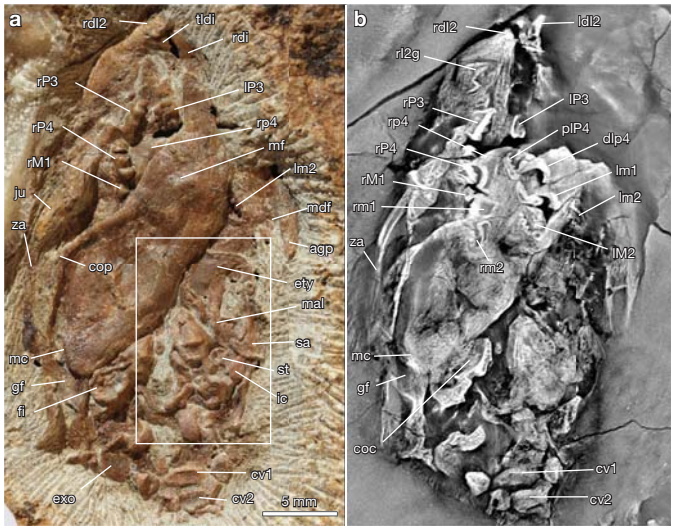

Figure 2 | Skull of *A. allinhopsoni* (holotype; HG-M017-A). **a**, Optic image of the skull in ventrolateral view (right mandible in lateral view). **b**, Computed laminography image of the skull. agp, angular process; coc, cochlear canal; cop, coronoid process; cv1, first cervical vertebra; cv2, second cervical vertebra; dlp4, distal portion of left fourth lower premolar; ety, ectotympanic (tympanic); exo, exoccipital; fi, fossa incudis (in epitympanic recess); gf, glenoid fossa; ic, incus; ju, jugal; ldI2, left second upper deciduous incisor; lm1, left first lower molar; lm2, left second lower molar; lM2, left second upper molar; lP3, left third upper premolar; mal, malleus; mc, mandibular condyle; mdf, mandibular foramen; mf, mental foramen; plP4, partial left fourth upper premolar; rdi, right lower deciduous incisor; rdI2, right second upper deciduous incisor; rl2g, germ of right second upper incisor; rm1, right first lower molar; rm2, right second lower molar; rM1, right first upper molar; rP3, right third upper premolar; rp4, right fourth lower premolar; rP4, right fourth upper premolar; sa, surangular; st, stapes; tldi, tip of left lower deciduous incisor; za, zygomatic arch. An expanded view of the box in **a** is shown in Extended Data Fig. 5. See Supplementary Information for discussion. Scale bar applies to both **a** and **b**.

long, proportionally shorter than that of *A. jenkinsi*, and is 3.9% of the skull length (30.8 mm), falling into the percentage range of the stapes/skull length ratio in mammals[7,8].

Lateral to the stapes, the incus body bears a convex articular surface for the malleus. Its long crus is robust compared to that of extant mammals[9,10], and extends anteromedially and tapers distally; its tip bends medially and ends as the lenticular process that articulates with the head of the stapes. The lateral side of the incus body appears to be in contact with the squamosal, which forms the lateral wall of the epitympanic recess.

Anterior to the stapes and incus are three bones, identified as the malleus, surangular, and ectotympanic. The malleus is dorsal to the surangular and ectotympanic, and its posterior portion is plate-like and delimited posteriorly by a curved ridge. This part is interpreted as the transverse part of the malleus, as in *Ornithorhynchus*[11]. The incudal facet of the malleus is probably on the dorsal side of the transversal part. At the anteromedial end of the transverse part, a bony prong projecting laterally is identified as the manubrium. Anterior to the manubrium is a robust process, a feature unknown on the malleus of mammals[9,10]; we term it the medial process of the malleus and consider it homologous to the retroarticular process of the articular. On the lateral side, the anterior process of the malleus is not fully exposed, but computed laminography images reveal a slim and relatively short process that adjoins the anterior process of the surangular. The bone identified as the surangular has a fan-shaped body and an anterior process that tapers anteriorly (Fig. 2; Extended Data Fig. 5). The body lies ventral to the transversal part of the malleus and is positioned closely medial to the glenoid fossa. Its posterior edge thickens as a curved ridge, and the smooth posterior surface is reminiscent of an articular surface. Judging from their similar shape, the dorsal side of the surangular body is likely to have been lodged in the concave area on the ventral side of the transversal part of the malleus in life. The ectotympanic is a thin plate without an anterior limb. As preserved, its medial portion forms a broad process that extends posteriorly and is interpreted as homologous to the reflected lamina of the angular in non-mammalian cynodonts. The anterior border of the plate thickens to form a low curved ridge.

As in other euharamiyidans[1,2], the skeletons of *A. allinhopsoni* have seven cervical, thirteen thoracic, six lumbar and three sacral vertebrae, and a long tail. The gracile skeleton shows arboreal adaptation in having slim ribs, a short pelvic girdle, and proportionally elongate and slim limbs. The scapula is rectangular, with the glenoid fossa roughly perpendicular to the long axis of the bone. The scapular spine was broken but its base shows that it extends diagonally on the scapular blade, with a small supraspinous fossa on the cranial side of the spine. The ulna and radius are longer than the humerus, and the tibia and fibula are longer than the femur (Extended Data Table 1). Typically for euharamiyidans[1–4], the metapodials are proportionally shorter than phalanges in both the pes and manus (Extended Data Figs 2, 3, 6 and 7).

Both type specimens have preserved impressions of the gliding membrane (patagium), with the paratype displaying some details of hair pattern as well as a carbonized substance that may be skin remains (Figs 1, 3; Extended Data Figs 2, 3 and 6). The impression shows that the gliding membrane attaches to the wrist and ankle region, as in many extant gliding mammals[12]. The primary gliding membrane (plagiopatagium) extends between the forelimb and hind limb, whereas the propatagium exists between the neck and forelimb and the uropatagium is between the hind limb and the tail. Similar to gliding mammals[12], the long tail bears dense hair that spreads broadly and is laterally bristled.

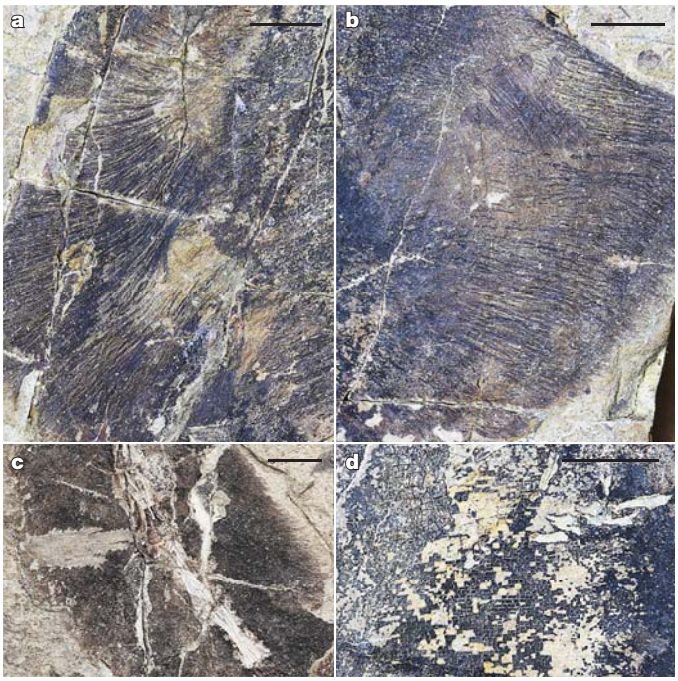

Figure 3 | Close-up views of impressions of fur and gliding membrane in *A. allinhopsoni* (paratype; HG-M018). a, **b**, Impressions of long and bristle-like hair on the gliding membrane that display some regular arrangement (corresponding to areas 1 and 2 in Fig. 1b). **c**, The tail bears dense hair that spreads broadly and laterally bristled (corresponding to box 3 in Fig. 1b). **d**, Carbonized substance that may be derived from the skin and/or muscle of the gliding membrane (corresponding to box 4 in Fig. 1b). Magnification is slightly different among panels. Scale bar in each panel, 5 mm.

There is no evidence for a calcar or any extra element at the wrist, elbow, or ankle that may serve as winglets, a structure commonly present in gliding mammals[12–14], but a bony spur is preserved in the paratype.

Phylogeny

Reiterating other studies[1,2,15–17], our phylogenetic analyses grouped 'haramiyidans' and multituberculates into a clade that is nested within Mammalia (Fig. 4; Extended Data Fig. 8), contrasting to alternative hypotheses[4,18]. In phylogenetic results based on parsimony (see Methods), *Haramiyavia* and *Thomasia* are basal to the clade consisting of multituberculates and euharamiyidans, whereas Bayesian analyses cluster *Haramiyavia* and *Thomasia* as a sister-group to other haramiyidans; the clade of haramiyidans further groups with multituberculates.

One of the hypotheses deemed that haramiyidans were members of the multituberculate stock, either as direct ancestors or an early side branch[19] (Supplementary Information). Our results based on parsimony encompass both possibilities: euharamiyidans probably represent an early side branch of multituberculates, and both groups were derived from a common ancestor similar to *Haramiyavia* and *Thomasia*, with euharamiyidans adapted to arboreal life and multituberculates to terrestrial life. By contrast, the Bayesian results identified a monophyletic Haramiyida, although the support for the clade is not robust. This phylogenetic result allows for the possibility that possession of the postdentary trough in *Haramiyavia*[18,20] represents a reversal within allotherians or that the definitive mammalian middle ear (DMME)[21,22] in euharamiyidans and multituberculates evolved independently. In general, however, the auditory apparatus of *A. allinhopsoni* and our phylogenetic results support the idea that the DMME evolved more than once[2,10,16,18,21–23] instead of only once[24–27] (Fig. 5). It is also clear that gliding locomotion evolved independently in two Jurassic groups as well as in several therian clades (Fig. 4).

Discussion

Auditory apparatus

The complete detachment of the auditory bones from the dentary in *A. allinhopsoni* confirms the interpretation made for other euharamiyidans[1,2,7] but differs from the reconstructed middle ear of *Vilevolodon*[4]. The morphologies of the ear bones of *A. allinhopsoni* differ from those of the transitional mammalian middle ear (TMME)[16] and the DMME[9,10,21,22] (Fig. 5). Specifically, the stapes of *Arboroharamiya* has a large process on the posterior crus that was considered homologous with the proximal end of the interhyal and functioned for the attachment of a sizable stapedius muscle in life[7]. The incus is likely to have been dorsal to the malleus in anatomic position, as in *Ornithorhynchus*[11], but differs from the latter in that its body is not a small plate but has a convex articular surface for the malleus, reminiscent of the articular–quadrate jaw articulation in non-mammalian cynodonts[21,28]. In therians, the incus has a saddle-shaped articular facet; the long crus of the incus with a lenticular process in *A. allinhopsoni* approaches the morphology of the therian incus[9,10]. This structure would enhance middle ear leverage for transmitting airborne sound vibrations from the tympanic membrane to the inner ear. It represents a derived condition compared to the quadrate in the mandibular middle ear (MdME) of *Morganucodon*[29] and the TMME[16] (Fig. 5).

The malleus bears the manubrium, which is the earliest known among mammaliaforms. Its shape and relationship with the other part of the malleus support the notion that the manubrium is a neomorphic outgrowth[16,21,30,31]. This unique long medial process probably functioned to frame part of the tympanic membrane in life. The anterior process of the malleus is relatively short, compared to those of many other mammals[9,10,16] (Fig. 5), and we postulate that it is partly homologous to the prearticular of non-mammalian cynodonts or the gonial in extant mammals[21,22,30–33].

The plate-like ectotympanic of *A. allinhopsoni* differs from those found in extant mammals[9,10], multituberculates[25,27], and the eutriconodontan *Liaoconodon*[16], which are sickle-shaped with a tympanic sulcus for holding the tympanic membrane. It also differs from the reconstructed slim reflected lamina in *Morganucodon*[21] and *Vilevolodon*[4]. The lack of the anterior limb of the ectotympanic, associated with the lack of the internal groove on the dentary, a short anterior process of the malleus, and distantly separated lower jaw and ear bones, demonstrates the full detachment of the auditory bones from the dentary. Because the tympanic sulcus is not developed, the tympanic membrane probably covered the ectotympanic ventrally and attached along the anterior ridge on the bony plate in life. This suggests that in the MdME, the tympanic membrane could have overlaid the lateral surface of the reflected lamina.

The surangular is unknown in any mammals that have a DMME or TMME, although a process at the rear of the malleus was interpreted as homologous to the surangular boss in *Liaoconodon*[16]. Of the four postdentary bones in non-mammalian cynodonts, the articular, prearticular and angular were transformed into the basicranial region and functioned exclusively for hearing in mammals[21,22,30–34], but the fate of the surangular seems to have been overlooked[16]. The surangular, as a major part of the postdentary complex, was present in basal mammaliaforms[21,22] such as *Morganucodon*[35] and *Haldanodon*[36]. In some advanced cynodonts, a subsidiary articulation between the surangular and the squamosal was developed and functioned to reduce the compressive load borne by the quadrate[21,22,28,37,38]. This articulation was considered as an intermediate stage in the development of the mammalian jaw joint, and the final stage in the evolution of this joint was thought to be exemplified by morganucodontids, in which the dentary condyle excluded the surangular from the joint[38]. The convex posterior end of the surangular in *A. allinhopsoni* is probably a remnant of the surangular boss for articulation with the initial glenoid fossa on the medial aspect of the squamosal rim, as in some non-mammalian cynodonts[21,38]. If this interpretation is correct, it corroborates the

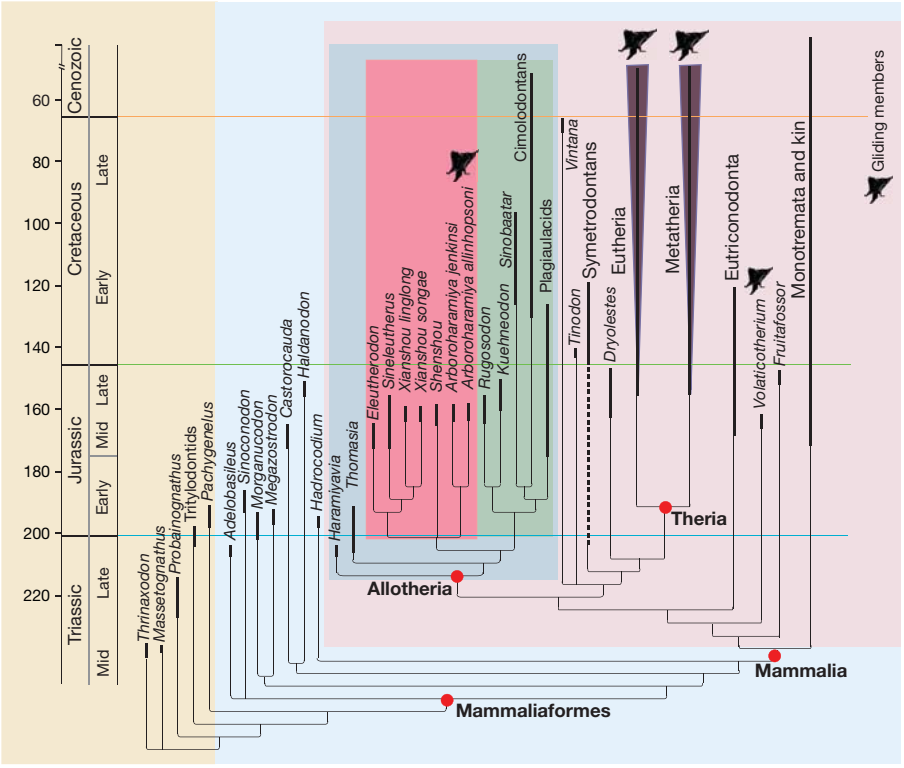

Figure 4 | Phylogeny of mammaliaformes with focus on Allotheria. This simplified phylogeny is based on the strict consensus tree that resulted from parsimony analyses (Extended Data Fig. 8a; Supplementary Information). Multituberculates and haramiyidans form the clade of allotherians that is nested within Mammalia. Euharamiyidans and multituberculates pair as a sister group, with *Haramiyavia* and *Thomosia* being outside as the stem taxa. As shown in the tree, gliding locomotion has evolved independently in extant mammals[12,14] and two distantly related Mesozoic taxa from the Yanliao Biota. See Methods, Extended Data Fig. 8, and Supplementary Information for more discussions.

hypothesis that the dentary condyle excluded the surangular from the craniomandibular joint in the development of the exclusive dentary–squamosal jaw joint (DSJJ) along with the formation of the DMME in mammals[38]. In some extant mammals, a small bone lying above the anterior process of the malleus, the accessory malleus (ossiculum accessorium mallei), has been proposed to be homologous to the surangular[39], but there seems to be no solid evidence to confirm this[30,31,40].

The evolution of the DMME coincided with formation of the DSJJ[21,22,28,31,37,38,41]. Our discovery raises the important issue of how the two systems co-evolved in allotherians that presumably had a palinal (posterior) jaw move during chewing, in contrast to the hinge jaw joint (HJJ; Fig. 5), which rotates at the articulation in mammaliaforms that have a triconodont tooth pattern or its derivatives. The evolution of the DMME would require different processes for detachment of the postdentary bones, depending on whether it evolved before or after the formation of the palinal jaw joint (PJJ). If *Haramiyavia* had the dual jaw joint (DJJ) and was capable of a palinal jaw movement[18], the DMME in euharamiyidans and/or multituberculates must have evolved after acquisition of the PJJ under the current phylogeny (Fig. 4; Extended Data Fig. 8a). In this case, the evolutionary transition from the postdentary bones to the ear ossicles would have had to cope with the palinal move of the DSJJ in allotherians. How the MdME in *Haramiyavia*[18,20] and *Vilevolodon*[4] functioned during this transition remains to be explained. Because the jaw move was also interpreted as being mainly orthal in *Haramiyavia*[6,20], the possibility that the PJJ evolved after detachment of the postdentary bones in allotherians cannot be ruled out.

Gliding

Gliding as a special type of locomotion exists in at least 64 species of extant marsupials, rodents, and dermopterans[12,14]. Their diversity and distributions have been interpreted as being related to structures of forests[42], although the relationship between habitat structure and gliding behaviour may be complex[43,44]. There are over 80 fossil mammal gliders, but their identification is debatable[14]. Only three Mesozoic gliding mammals have been identified—*Volaticotherium antiquum*[45], *Maiopatagium*[3] and *Vilevolodon*[4]—all from the Jurassic Yanliao biota. Although these mammals share similar structures for gliding adaptation, such as a gracile skeleton, elongation of limbs, and development of the gliding membrane, they differ in several aspects. Unlike *V. antiquum*, the pes and manus of euharamiyidans have elongated phalanges but relatively short metapodials. The gliding membrane of *V. antiquum* appears to be larger and bears finer hair than that of euharamiyidans; the latter is more similar to those of extant gliding therians[12] in bearing long and bristle-like hairs that show some pattern of arrangement[46].

A long tail with long hair has been hypothesized to serve for counterbalancing or manoeuvring in gliding[47], and the gliding membrane is a complex system, consisting of muscular sheets associated with the neck, limbs, and tail[13,44,48] and rope-like muscles extending along the edges of the membrane[13]; these muscles are used for control of the membrane during flight and for holding the membranes against the body during quadrupedal locomotion[44]. A similar muscular system could be inferred for the Jurassic gliding euharamiyidans. On the basis of skeletal evidence, an arboreal lifestyle has been suggested to have been common in euharamiyidans[1,2]. Because of their similar skeletal features, it is likely that gliders were common in euharamiyidans. This indicates that euharamiyidans represent a major mammalian group adapted to arboreal life and gliding locomotion in Jurassic forests, independent of *Volaticotherium*. The arboreal experiment may have actually started in the Late Triassic *Haramiyavia*, which has a gracile skeleton and relatively long radius and distal limb, compared to those of *Morganucodon*[20].

Early mammals are considered to have been nocturnal[38]. A nocturnal life may be inferred for euharamiyidans, because all species of extant

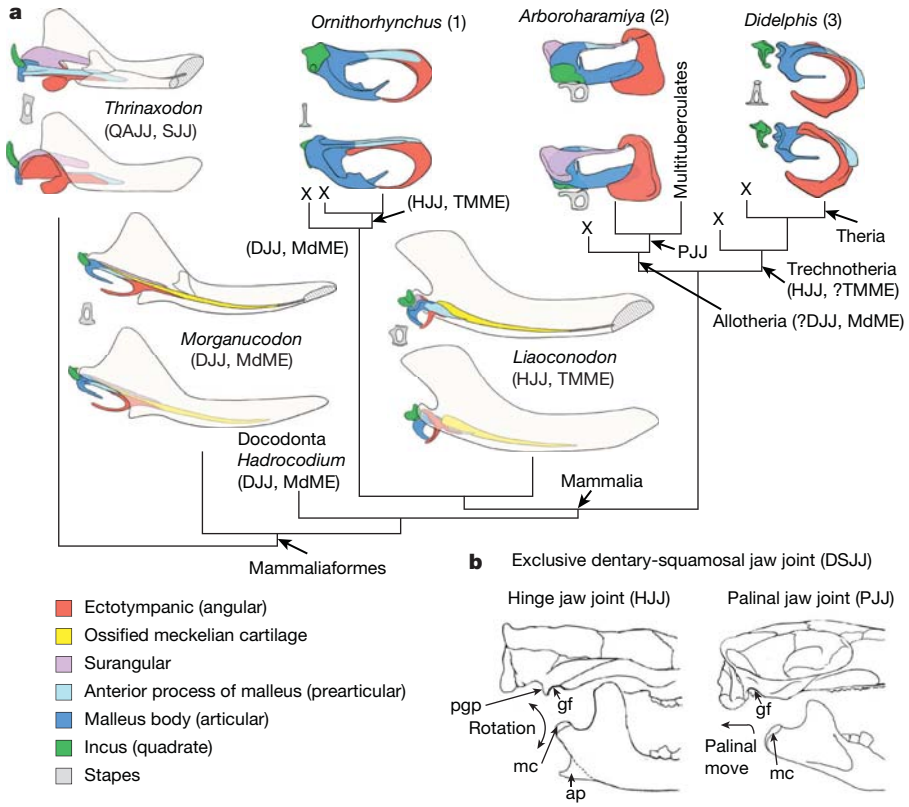

Figure 5 | Comparison of mammaliaform middle ears and jaw joints. **a**, Different types of auditory bones mapped on a simplified phylogeny. **b**, Sketches showing two exclusive dentary–squamosal jaw joints in mammals. ap, angular process; DJJ, Dual jaw joint; MdME, mandibular middle ear; pgp, postglenoid process; QAJJ, quadrate–articular jaw joint; SJJ, subsidiary jaw joint (between the surangular and squamosal); TMME, transitional mammalian middle ear; X, stem taxa to clade with definitive mammalian middle ear (DMME). 1, DMME in monotremes as represented by *Ornithorhynchus*. 2, DMME in *Arboroharamiya*. 3, DMME in therians as represented by *Didelphis*. Some auditory bone images have been flipped for convenient comparison. For each pair of auditory bones, the upper is medial view and the lower is lateral view (dorsal and medial, respectively, for *Arboroharamiya* and *Ornithorhynchus*) and the anterior is to the right in all. Dentary in lateral view is drawn semi-transparent to show postdentary complex or ear structure. Figure sources are from ref. 21 for *Thrinaxodon*, *Morganucodon*, and *Didelphis* (with permission from John Wiley and Sons) and from ref. 11 for *Ornithorhynchus* (with permission from Springer Nature). See Methods and Supplementary Information for explanations and additional information regarding figure sources.

gliding mammals are nocturnal[12]. The gliding *A. allinhopsoni* and other species[3,4] add to the diversity and disparity of Jurassic mammals[49,50] and support the notion that a major adaptive radiation of mammals took place in the Middle–Late Jurassic[51,52]. As one of the earliest known groups of mammals, the poor fossil record of haramiyidans may be attributed to their gracile skeleton and arboreal life in a forest environment, which were unfavourable for fossil preservation[51]. As tree dwellers, the extinction of euharamiyidans was possibly caused by the change from gymnosperm-dominant forests to an ecosystem in which angiosperms flourished during the Jurassic–Cretaceous transition[50].

Online Content Methods, along with any additional Extended Data display items and Source Data, are available in the online version of the paper; references unique to these sections appear only in the online paper.

Received 16 February; accepted 3 October 2017.
Published online 13 November 2017.

1. Zheng, X., Bi, S., Wang, X. & Meng, J. A new arboreal haramiyid shows the diversity of crown mammals in the Jurassic period. *Nature* **500,** 199–202 (2013).
2. Bi, S., Wang, Y., Guan, J., Sheng, X. & Meng, J. Three new Jurassic euharamiyidan species reinforce early divergence of mammals. *Nature* **514,** 579–584 (2014).
3. Meng, Q. J. *et al.* New gliding mammaliaforms from the Jurassic. *Nature* **548,** 291–296 (2017).
4. Luo, Z. X. *et al.* New evidence for mammaliaform ear evolution and feeding adaptation in a Jurassic ecosystem. *Nature* **548,** 326–329 (2017).
5. Fox, R. C. & Meng, J. An X-radiographic and SEM study of the osseous inner ear of multituberculates and monotremes (Mammalia): implications for mammalian phylogeny and evolution of hearing. *Zool. J. Linn. Soc.* **121,** 249–291 (1997).
6. Kielan-Jaworowska, Z., Cifelli, R. L. & Luo, Z.-X. *Mammals from the Age of Dinosaurs: Origins, Evolution, and Structure* (Columbia Univ. Press, 2004).
7. Meng, J., Bi, S., Zheng, X. & Wang, X. Ear ossicle morphology of the Jurassic euharamiyidan *Arboroharamiya* and evolution of mammalian middle ear. *J. Morphol.* http://doi.org/10.1002/jmor.20565 (2016).
8. Wible, J. R. Origin of Mammalia: the craniodental evidence reexamined. *J. Vertebr. Paleontol.* **11,** 1–28 (1991).
9. Doran, A. H. G. Morphology of the mammalian ossicular auditûs. *Trans. Linn. Soc. Lond* **1,** 371–497 (1878).
10. Fleischer, G. Studien am Skelett des Gehörorgans der Säugetiere, einschließlich des Menschen. *Saugetierkdl. Mitt.* **21,** 131–239 (1973).
11. Zeller, U. in *Mammal Phylogeny: Mesozoic Differentiation, Multituberculates, Monotremes, Early Therians, and Marsupials* (eds Szalay, F. S., Novacek, M. J. & McKenna, M. J.) 95–107 (Springer, 1993).
12. Jackson, S. & Schouten, P. *Gliding Mammals of the World* (CSIRO, 2012).
13. Johnson-Murray, J. L. The comparative myology of the gliding membranes of *Acrobates, Petauroides* and *Petaurus* contrasted with the cutaneous myology of *Hemibelideus* and *Pseudocheirus* (Marsupialia: Phalangeridae) and with selected gliding Rodentia (Sciuridae and Anamoluridae). *Aust. J. Zool.* **35,** 101–113 (1987).
14. Jackson, S. M. & Thorington, R. W. Jr. Gliding mammals: taxonomy of living and extinct species. *Smithson. Contrib. Zool.* **638,** 1–117 (2012).
15. Luo, Z.-X., Yuan, C.-X., Meng, Q.-J. & Ji, Q. A Jurassic eutherian mammal and divergence of marsupials and placentals. *Nature* **476,** 442–445 (2011).
16. Meng, J., Wang, Y. & Li, C. Transitional mammalian middle ear from a new Cretaceous Jehol eutriconodont. *Nature* **472,** 181–185 (2011).
17. Krause, D. W. *et al.* First cranial remains of a gondwanatherian mammal reveal remarkable mosaicism. *Nature* **515,** 512–517 (2014).
18. Luo, Z.-X., Gatesy, S. M., Jenkins, F. A. Jr, Amaral, W. W. & Shubin, N. H. Mandibular and dental characteristics of Late Triassic mammaliaform *Haramiyavia* and their ramifications for basal mammal evolution. *Proc. Natl Acad. Sci. USA* **112,** E7101–E7109 (2015).
19. Hahn, G. Neue Zähne von Haramiyiden aus der deutschen Ober-Trias und ihre Beziehungen zu den Multituberculaten. *Palaeontogr. Abt. A* **142,** 1–15 (1973).

20. Jenkins, F. A., Jr, Gatesy, S. M., Shubin, N. H. & Amaral, W. W. Haramiyids and Triassic mammalian evolution. *Nature* **385,** 715–718 (1997).
21. Allin, E. F. Evolution of the mammalian middle ear. *J. Morphol.* **147,** 403–437 (1975).
22. Allin, E. F. & Hopson, J. A. in *The Evolutionary Biology of Hearing* (eds Webster, D. B., Popper, A. N. & Fay, R. R.) 587–614 (Springer, 1992).
23. Rich, T. H. *et al.* The mandible and dentition of the Early Cretaceous monotreme *Teinolophos trusleri*. *Alcheringa* **40,** 475–501 (2016).
24. Presley, R. Lizards, mammals and the primitive tetrapod tympanic membrane. *Symp. Zool. Soc. Lond.* **52,** 127–152 (1984).
25. Meng, J. & Wyss, A. R. Monotreme affinities and low-frequency hearing suggested by multituberculate ear. *Nature* **377,** 141–144 (1995).
26. Hurum, J. H., Presley, R. & Kielan-Jaworowska, Z. The middle ear in multituberculate mammals. *Acta Palaeontol. Pol.* **41,** 253–275 (1996).
27. Rougier, G. W., Wible, J. R. & Novacek, M. J. Middle-ear ossicles of the multituberculate *Kryptobaatar* from the Mongolian Late Cretaceous: implications for mammaliamorph relationships and the evolution of the auditory apparatus. *Am. Mus. Novit.* **3187,** 1–43 (1996).
28. Kemp, T. S. Acoustic transformer function of the postdentary bones and quadrate of a nonmammalian cynodont. *J. Vertebr. Paleontol.* **27,** 431–441 (2007).
29. Kermack, K. A., Mussett, F. & Rigney, H. W. The skull of *Morganucodon*. *Zool. J. Linn. Soc.* **71,** 1–158 (1981).
30. Mallo, M. Formation of the middle ear: recent progress on the developmental and molecular mechanisms. *Dev. Biol.* **231,** 410–419 (2001).
31. Anthwal, N., Joshi, L. & Tucker, A. S. Evolution of the mammalian middle ear and jaw: adaptations and novel structures. *J. Anat.* **222,** 147–160 (2013).
32. Gaupp, E. Die Reichertsche Theorie (Hammer-, Amboss- und Kieferfrage). *Archiv. Anatomie. Entwick* **1912,** 1–426 (1913).
33. Maier, W. & Ruf, I. Evolution of the mammalian middle ear: a historical review. *J. Anat.* **228,** 270–283 (2016).
34. Reichert, C. Über die Visceralbogen der Wirbelthiere im Allgemeinen und deren Metamorphosen bei den Vögeln und Säugethieren. *Arch. Anat. Phys. Med.* **1837,** 120–220 (1837).
35. Kermack, K. A., Mussett, F. & Rigney, H. W. The lower jaw of *Morganucodon*. *Zool. J. Linn. Soc.* **53,** 87–175 (1973).
36. Lillegraven, J. A. & Krusat, G. Cranio-mandibular anatomy of *Haldanodon exspectatus* (Docodonta; Mammalia) from the Late Jurassic of Portugal and its implications to the evolution of mammalian characters. *Contrib. Geol* **28,** 39–138 (1991).
37. Crompton, A. W. in *Studies in Vertebrate Evolution* (eds Joysey, K. A. & Kemp, T. S.) 231–251 (Oliver & Boyd, 1972).
38. Crompton, A. W. & Jenkins, F. A. Jr in *Mesozoic Mammals: The First Two-thirds of Mammalian History* (eds Lillegraven, J. A., Kielan-Jaworowska, Z. & Clemen, W. A.) 59–73 (Univ. California Press, 1979).
39. Henson, O. W. Jr. in *The Handbook of Sensory Physiology: the Auditory System VII* (eds Keidel, W. D. & Neff, W. D.) 39–110 (Springer, 1974).
40. Tucker, A. S., Watson, R. P., Lettice, L. A., Yamada, G. & Hill, R. E. Bapx1 regulates patterning in the middle ear: altered regulatory role in the transition from the proximal jaw during vertebrate evolution. *Development* **131,** 1235–1245 (2004).
41. Crompton, A. W. & Hylander, W. L. in *The Ecology and Biology of Mammal-like Reptiles* (eds Hotton, N. III, MacLean, P. D., Roth J. J. & Rot E. C.) 263–282 (Smithsonian Inst. Press, 1986).
42. Dial, R., Bloodworth, B., Lee, A., Boyne, P. & Heys, J. The distribution of free space and its relation to canopy composition at six forest sites. *For. Sci.* **50,** 312–325 (2004).
43. Heinicke, M. P., Greenbaum, E., Jackman, T. R. & Bauer, A. M. Evolution of gliding in Southeast Asian geckos and other vertebrates is temporally congruent with dipterocarp forest development. *Biol. Lett.* **8,** 994–997 (2012).
44. Socha, J. J., Jafari, F., Munk, Y. & Byrnes, G. How animals glide: from trajectory to morphology. *Can. J. Zool.* **93,** 901–924 (2015).
45. Meng, J., Hu, Y., Wang, Y., Wang, X. & Li, C. A Mesozoic gliding mammal from northeastern China. *Nature* **444,** 889–893 (2006).
46. Hayssen, V. Patterns of body and tail length and body mass in Sciuridae. *J. Mamm.* **89,** 852–873 (2008).
47. Dudley, R. *et al.* Gliding and the functional origins of flight: biomechanical novelty or necessity? *Annu. Rev. Ecol. Evol. Syst.* **38,** 179–201 (2007).
48. Endo, H., Yokokawa, K., Kurohmaru, M. & Hayashi, Y. Functional anatomy of gliding membrane muscles in the sugar glider (*Petaurus breviceps*). *Ann. Anat.* **180,** 93–96 (1998).
49. Luo, Z.-X. Transformation and diversification in early mammal evolution. *Nature* **450,** 1011–1019 (2007).
50. Grossnickle, D. M. & Polly, P. D. Mammal disparity decreases during the Cretaceous angiosperm radiation. *Proc. R. Soc. Lond. B* **280,** 20132110 (2013).
51. Meng, J. Mesozoic mammals of China: implications for phylogeny and early evolution of mammals. *Natl Sci. Rev.* **1,** 521–542 (2014).
52. Close, R. A., Friedman, M., Lloyd, G. T. & Benson, R. B. Evidence for a mid-Jurassic adaptive radiation in mammals. *Curr. Biol.* **25,** 2137–2142 (2015).

Supplementary Information is available in the online version of the paper.

Acknowledgements We thank S.-H. Xie for specimen preparation; P.-F. Yin and Y.-M. Hou for computed laminography scanning of the specimens; X.-T. Zheng, X.-L. Wang, H.-J. Li, Z.-J. Gao, X.-H. Ding, and D.-Y. Sun for access to comparative specimens; N. Wong for drawing the auditory bones and animal reconstruction; D. W. Krause and S. Hoffmann for sharing data and insights on incisor identification; D. Sigogneau-Russell and Z.-X. Luo for permissions to use their published figures; and Z.-X. Luo, Z.-H. Zhou, X. Xu, G. Rougier, J. A. Schultz, A. S. Tucker, and M. Takechi for discussions. This work was supported by the National Natural Science Foundation of China (41688103; 41404022) and the Strategic Priority Research Program (B) of the Chinese Academy of Sciences (XDB18000000).

Author Contributions G.H. and J.M. conceived the study. G.H. acquired and curated the specimens and did the field investigation. F.M. conducted computed laminography, rendered the data, and did most of the phylogenetic analyses and figures. S.B., Y.W. and F.M. helped to build the character list. J.M. supervised preparation of the specimen and design of the figures and drafted the manuscript; all authors edited and approved the manuscript.

Author Information Reprints and permissions information is available at www.nature.com/reprints. The authors declare no competing financial interests. Readers are welcome to comment on the online version of the paper. Publisher's note: Springer Nature remains neutral with regard to jurisdictional claims in published maps and institutional affiliations. Correspondence and requests for materials should be addressed to F.M. (maofangyuan@ivpp.ac.cn) or J.M. (jmeng@amnh.org).

Reviewer Information *Nature* thanks G. Rougier and the other anonymous reviewer(s) for their contribution to the peer review of this work.

METHODS

Specimen preparation. The skull embedded in the main slab (holotype, HG-M017-A) was needle prepared from the backside of the slab. The preparation revealed the complete right mandible with the upper and lower teeth in natural occlusion; it also revealed most of the basicranial region, including both occipital condyles, both promontorii, and the left ear region with auditory bones preserved in nearly original position. The manus and pes were embedded in the counterpart (HG-M017-B) and needle preparation exposed the bones in ventral view.

Measurements. The skeletal elements were measured using a digital caliper. The measurement for each element was repeated three times, and the average was used. The measurements are listed in Extended Data Table 1.

Imaging and figures. Optical images were taken using a Canon Digital camera with a macro lens. Because of the flat preservation of the specimens on large rock slabs, computed laminography was used to enhance observation of the morphology of the crushed specimens. The scanner was developed by the Institute of High Energy Physics, Chinese Academy of Sciences (CAS) and has been installed at the Key Laboratory of Vertebrate Evolution and Human Origins, Chinese Academy of Sciences, where the scanning was carried out. The specimens were scanned with a beam energy of 60 kV and a flux of 40 μA, using a 360° rotation with a step size of 1°. A total of 360 image slices with a resolution of 2,048 by 2,048 pixels were obtained using a modified Feldkamp algorithm. The resolution of the computed laminography scan for the holotype (HG-M017) is 28.1 μm per pixel for the skull, 8.7 μm per pixel for ear area, and 84.5 μm per pixel for the skeleton. The resolution for the skeleton of the paratype (HG-M018) is 61.26 μm per pixel.

Some ear bone figures in Fig. 5 were redrawn. The stapes for *Morganucodon* and *Thrinaxodon* is based on ref. 21. The distal portion of the stapes was not preserved in *Morganucodon*[29] but was reconstructed; whether there was a process for insertion of the stapedius muscle remains unknown. The stapes of *Liaoconodon* is borrowed from *Chaoyangodens*[53]. Other figures are based on the following studies: *Thrinaxodon*, *Morganucodon,* and *Didelphis* from ref. 21 (with permission from John Wiley and Sons), *Ornithorhynchus* from ref. 11 (with permission from Springer Nature), and *Liaoconodon* from ref. 16. The interpretations of jaw and middle ear structures, such as the surangular and ossified Meckel's cartilage in relevant taxa, have been detailed elsewhere[16].

Taxa selected. The data matrix used in the phylogenetic analyses contains 117 taxa and 505 characters, and is built upon several other studies[1,2,54,55]. We have changed some taxa selected for phylogenetic analyses. Because of controversies regarding the morphology of *Megaconus*[54,56], we did not include this taxon in the present analysis. Instead, we added *Volaticotherium* and *Liaoconodon* to our analyses. *Volaticotherium*[45] is the only known Mesozoic gliding mammal from the Jurassic Yanliao biota[51,57,58] (but see the recently discovered *Maiopatagium*[3] and *Vilevolodon*[4] and related discussion in the Supplementary Information) and is possibly related to eutriconodontans[59,60]. The eutriconodontan *Liaoconodon* is from the Early Cretaceous Jehol biota, and in its holotype specimen the malleus, incus, ectotympanic, and ossified Meckel's cartilage are unequivocally preserved in articulation[16]. Inclusion of these two taxa in the phylogenetic analyses better reflects our knowledge about the evolution of gliding locomotion and the middle ear in early mammals. Finally, we added *Vintana*[17] to the data matrix upon the recommendation of a reviewer. Because there are two identifications of the premolar and molar of Gondwanatherian genera[17,61], the character coding for cheek teeth of *Vintana* is treated in two scenarios: *Vintana* A (with one premolar and four molars) and *Vintana* B (with three premolars and two molars)[17].

Taxonomic terminology. We follow the node-based crown clade concept for Mammalia, Monotremata, and Theria[62,63] instead of a more traditional definition of Mammalia[6]. The traditional definition of Mammalia is equivalent to Mammaliaformes[62,63]. In this study the term mammaliaforms is used to refer to animals in the taxon Mammaliaformes. We use Euharamiyida[2] for the clade that does not include some taxa traditionally placed in Haramiyida, such as *Haramiyavia* and *Thomasia*. We consider the clade Allotheria to consist of multituberculates and haramiyidans, but are aware of alternative hypotheses, such as that haramiyidans were placed outside of Mammalia[18], according to which the membership of Allotheria would be different. We also concur with the view that the traditional haramiyidans form a paraphyletic group[64–67], and have therefore placed the term in quotation marks at first use, although in our study a monophyletic group of haramiyidans has been recognized in Bayesian analyses (see discussion in Supplementary Information).

Characters and coding. We added ten new characters to the previous data matrix[2] and made changes on character codings that are supported by new evidence. For instance, the enamel microstructures for euharamiyidans have now become available[68] so that relevant characters can be coded accordingly. Similarly, features obtained from the computed laminography scan helped to improve some character codings of euharamiyidans. New data have also become available for other taxa, such as *Haramiyavia*[18], *Teinolophos*[23] and *Hadrocodium*[69], and modifications of character codings in these taxa have been made wherever necessary. In previous studies, some characters and character codings have been disputed[7,18,56]; these characters were further discussed in this study. To ensure maximum objectivity as we discuss the disputed characters and states, we follow previous studies[7,63] in using images to illustrate some of the character states in question. Character list and relevant discussions on disputed characters are presented in the character list in the Supplementary Information.

Phylogenetic analysis. Phylogenetic analyses were conducted using parsimony-based analyses in PAUP* (Version 4.0a152)[70] and likelihood-based Bayesian estimation in MrBayes v. 3.2.4[71,72]. We have run the two datasets (with *Vintana* A and *Vintana* B) for parsimony and Bayesian analyses. A heuristic search was conducted in the parsimony analyses, with the following settings: all characters (505) are parsimony-informative and unordered, and have equal weight; multistate taxa are interpreted as uncertainty; starting tree(s) is obtained via stepwise addition; addition sequence is random with starting seed generated automatically; tree bisection–reconnection (TBR) is used and set up with reconnection limit equal to eight; 'MulTrees' option is not in effect and one tree is saved per replicate; steepest descent option is not in effect; no topological constraint is in effect; trees are unrooted; number of replicates is 100,000. One thousand bootstrap replicates were run for the strict consensus tree and the bootstrap 50% majority-rule consensus trees for *Vintana*-A and *Vintana*-B datasets are presented in the Supplementary Information. For Bayesian analyses, we use the Mk model for discrete morphological data (data not partitioned, data type being standard, and coding being variable) and a gamma parameter for rate variation. Bayesian analyses were run for five million Markov chain Monte Carlo (MCMC) generations with the following settings: number of runs to 4, burn-in fraction to 0.25 (discarding the first 25% of sampled trees), sample frequency to 1,000, and number of chains to 4. The results of the phylogenetic analyses are presented in the Supplementary Information.

Data availability. The specimens (HG-M017, HG-M018) described in this study are archived in the Paleontology Center, Bohai University, Jinzhou, Liaoning Province, China. Supporting data (character list and data matrix) for phylogenetic analyses for this study are provided in the Supplementary Information. A Life Science Identifier (LSID) for the new species has been registered at ZooBank (http://zoobank.org/): urn:lsid:zoobank.org:act:F0BA37A9-0613-4BFE-8F26-43A17C85E409.

53. Meng, J. & Hou, S.-L. Earliest known mammalian stapes from an early cretaceous eutriconodontan mammal and implications for evolution of mammalian middle ear. *Palaeontol. Polonica* **67,** 181–196 (2016).
54. Zhou, C.-F., Wu, S., Martin, T. & Luo, Z.-X. A Jurassic mammaliaform and the earliest mammalian evolutionary adaptations. *Nature* **500,** 163–167 (2013).
55. Yuan, C.-X., Ji, Q., Meng, Q.-J., Tabrum, A. R. & Luo, Z.-X. Earliest evolution of multituberculate mammals revealed by a new Jurassic fossil. *Science* **341,** 779–783 (2013).
56. Meng, J., Bi, S., Wang, Y., Zheng, X. & Wang, X. Dental and mandibular morphologies of *Arboroharamiya* (Haramiyida, Mammalia): a comparison with other haramiyidans and *Megaconus* and implications for mammalian evolution. *PLoS One* **9,** e113847 (2014).
57. Zhou, Z.-H., Jin, F. & Wang, Y. Vertebrate assemblages from the middle-late Jurassic Yanliao Biota in Northeast China. *Earth Sci. Front* **17,** 252–254 (2010).
58. Xu, X., Zhou, Z.-H., Sullivan, C., Wang, Y. & Ren, D. An updated review of the Middle-Late Jurassic Yanliao biota: chronology, taphonomy, paleontology and paleoecology. *Acta Geol. Sin.* (English Edition) **90,** 2229–2243 (2016).
59. Gaetano, L. C. & Rougier, G. W. New materials of *Argentoconodon fariasorum* (Mammaliaformes, Triconodontidae) from the Jurassic of Argentina and its bearing on triconodont phylogeny. *J. Vertebr. Paleontol.* **31,** 829–843 (2011).
60. Gaetano, L. C. & Rougier, G. W. First amphilestid from South America: a molariform from the Jurassic Cañadón Asfalto Formation, Patagonia, Argentina. *J. Mamm. Evol.* **19,** 235–248 (2012).
61. Gurovich, Y. & Beck, R. The phylogenetic affinities of the enigmatic mammalian clade Gondwanatheria. *J. Mamm. Evol.* **16,** 25–49 (2009).
62. Rowe, T. Definition, diagnosis and origin of Mammalia. *J. Vertebr. Paleontol.* **8,** 241–264 (1988).
63. O'Leary, M. A. *et al.* The placental mammal ancestor and the post-K-Pg radiation of placentals. *Science* **339,** 662–667 (2013).
64. Butler, P. M. Review of the early allotherian mammals. *Acta Palaeontol. Pol.* **45,** 317–342 (2000).
65. Butler, P. M. & Hooker, J. J. New teeth of allotherian mammals from the English Bathonian, including the earliest multituberculates. *Acta Palaeontol. Pol.* **50,** 185–207 (2005).
66. Hahn, G. & Hahn, R. Evolutionary tendencies and systematic arrangement in the Haramiyida (Mammalia). *Geol. Palaeontol* **40,** 173–193 (2006).
67. Averianov, A. O. & Lopatin, A. V. Phylogeny of triconodonts and symmetrodonts and the origin of extant mammals. *Dokl. Biol. Sci.* **436,** 32–35 (2011).
68. Mao, F.-Y., Wang, Y.-Q., Bi, S.-D., Guan, J. & Meng, J. Tooth enamel microstructures of three Jurassic euharamiyidans and implications for tooth enamel evolution in allotherian mammals. *J. Vertebr. Paleontol.* **37,** e1279168 (2017).
69. Luo, Z.-X., Schultz, J. A. & Ekdale, E. G. in *Evolution of the Vertebrate Ear* (eds Clack, J. A., Fay, R. R. & Popper, A. N.) 139–174 (Springer, 2016).
70. Swofford, D. L. PAUP* - Phylogenetic analysis Using Parsimony (*and other methods). Version 4 (4.0a152) (Sinauer Associates, 2002).
71. Ronquist, F. & Huelsenbeck, J. P. MrBayes 3: Bayesian phylogenetic inference under mixed models. *Bioinformatics* **19,** 1572–1574 (2003).
72. Ronquist, F. *et al.* MrBayes 3.2: efficient Bayesian phylogenetic inference and model choice across a large model space. *Syst. Biol.* **61,** 539–542 (2012).

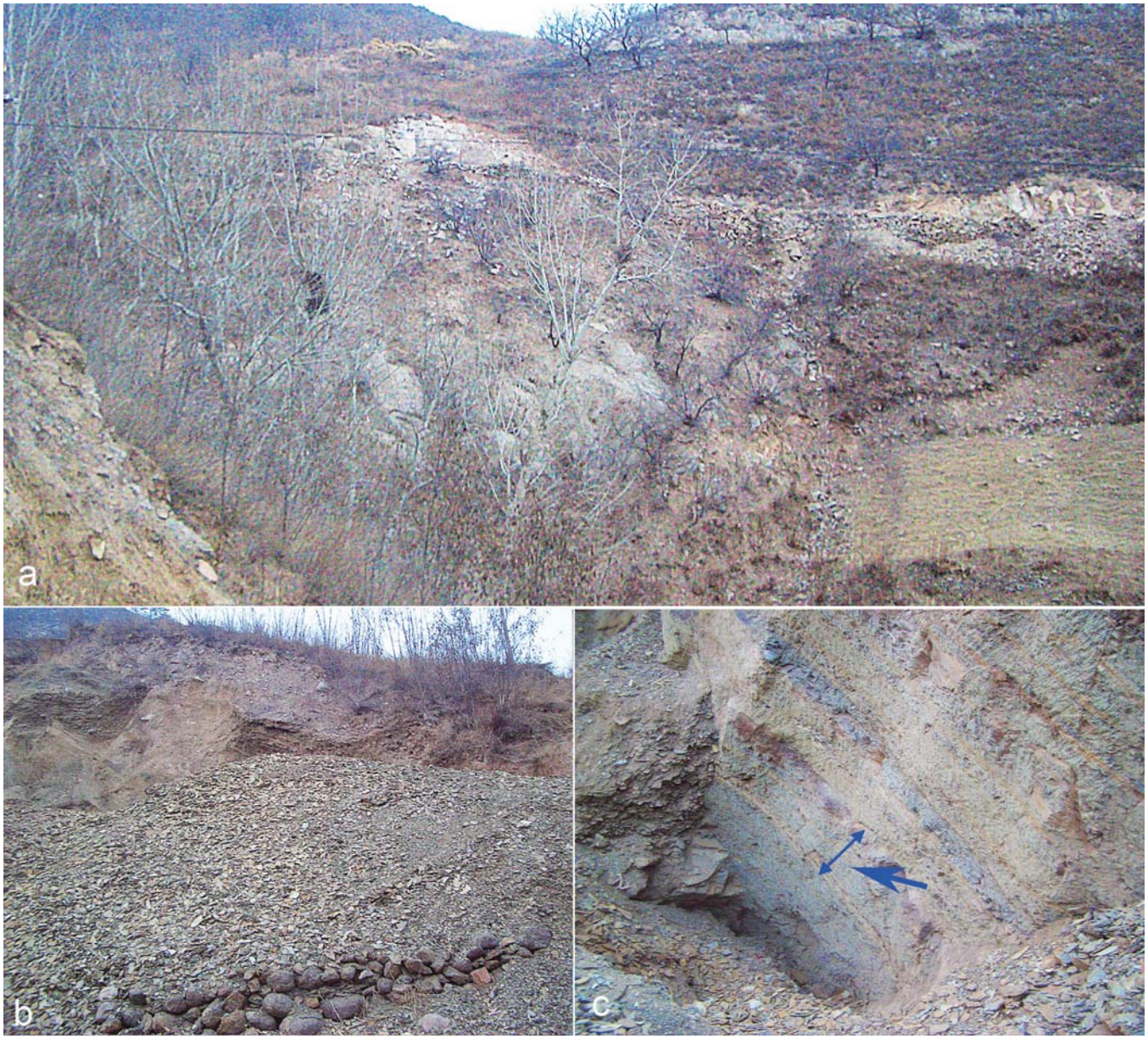

Extended Data Figure 1 | The type locality and fossil pit where the type specimens of *A. allinhopsoni* were collected. a, Distant view of the fossil locality and Tiaojishan Formation in the area of Nanshimen village, Gangou Town, Qinglong County, Hebei Province, China. **b**, **c**, The fossil pits where the type specimens were collected. The blue arrow in c points to the bed that generated the holotype and paratype. All photographs were taken by G.H. See Supplementary Information for more discussion on the age constraints of the beds and the fauna.

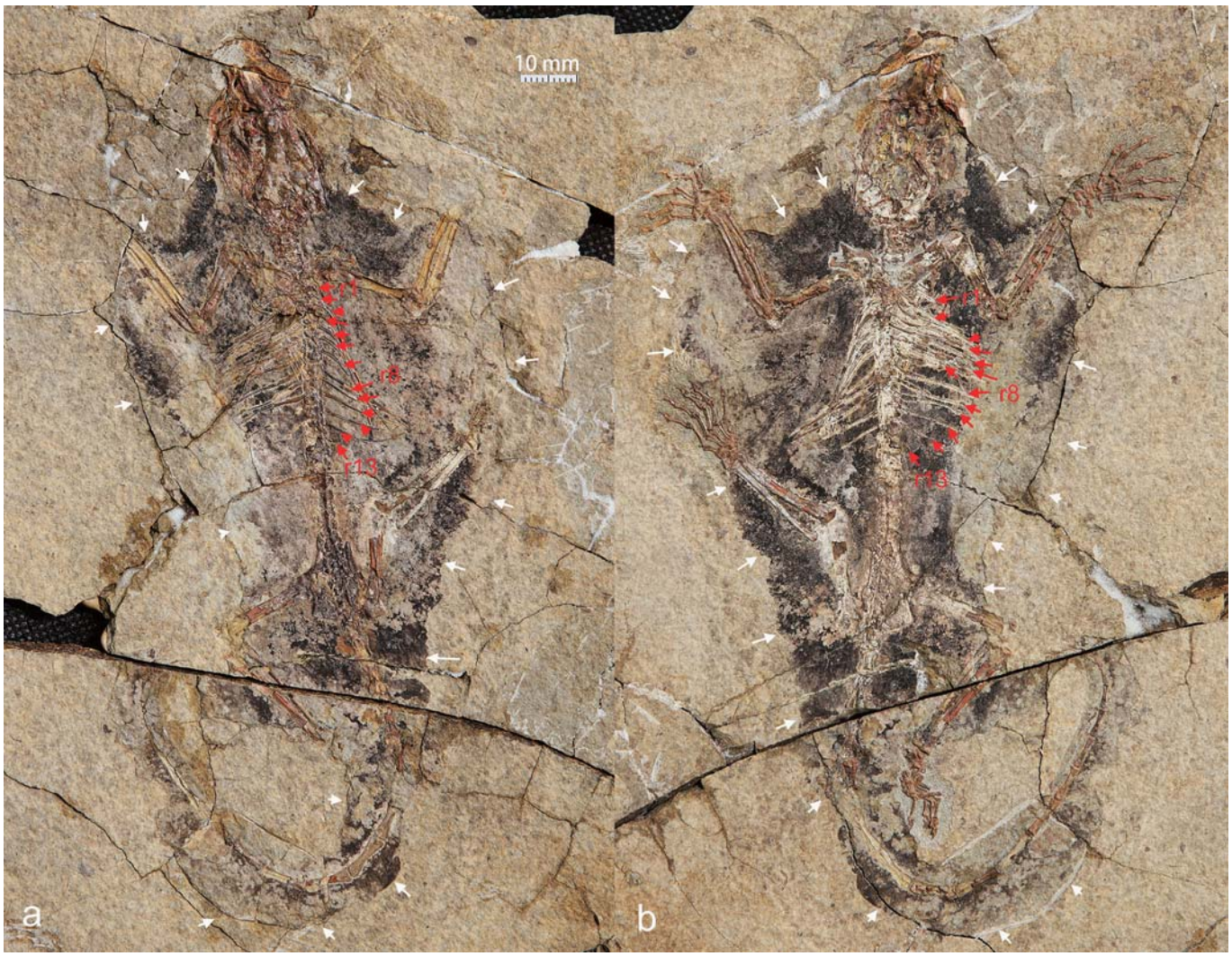

Extended Data Figure 2 | The holotype specimen (HG-M017) of *A. allinhopsoni*. The specimen preserves most of the skull, dentition, vertebral column and impressions of the gliding membrane and fur (dark colour). **a**, The main part of the holotype (HG-M017-A), in which the skull and vertebral column are exposed in their dorsal views (see also Figs 2, 3; Extended Data Fig. 4). **b**, The counterpart of the holotype (HG-M017-B), which preserves most of the limb structures and the molds of the vertebral column preserved in the main part. The limbs are exposed primarily in their ventral views (see also Extended Data Fig. 6). Red arrows point to ribs (1–13); white arrows mark the exposed edges of the gliding membrane.

Extended Data Figure 3 | The paratype specimen (HG-M018) of *A. allinhopsoni*. **a**, The main part of the paratype (HG-M018-A), which shows the ventral view of the skeleton (mainly the thoracic and lumbar vertebra) and impressions of the gliding membrane and body fur. **b**, The counterpart of the paratype (HG-M018-B). Skeletal remains preserved in the counterpart (peeled off from the main part) are mainly in the dorsal view. The skull was broken during excavation and reconstructed afterward; this area is outlined with a white dashed line to caution against potential misunderstanding of the morphology. The shape of the gliding membrane and impressions of hair are well preserved in the paratype and the exposed edge is marked by white arrows (see also Fig. 3; Extended Data Fig. 6a, b). The red arrows in **a** point to bony spurs[2]. The red arrows in **b** point to the ribs; 12 ribs can be recognized, but we assume there are a total of 13 ribs, as in the holotype specimen. **c**, Reconstruction of the animal in gliding motion.

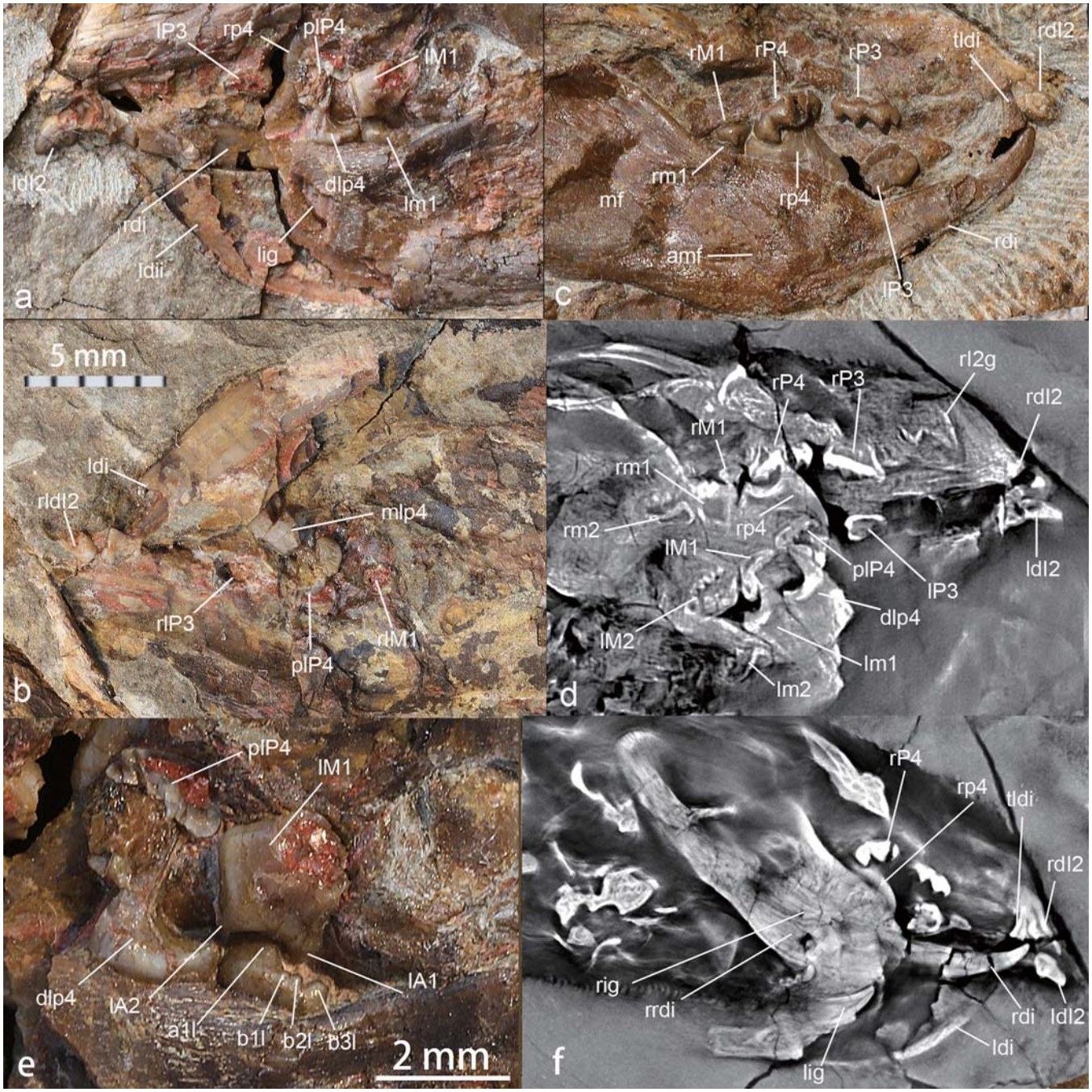

Extended Data Figure 4 | Dentition of *A. allinhopsoni* (holotype, HG-M017). a, Part of the skull with exposed teeth (HG-M017-A). **b**, Counterpart of the skull part in **a**. **c**, Part of the skull with teeth (HG-M017-A). This was prepared from the back side of the main slab. **d**, Computed laminography image that roughly corresponds to the area shown in **c**, revealing teeth within the maxilla and blocked by bones. **e**, Close-up view showing the occlusal relationship of M1 and m1. As in *A. jenkinsi* and other euharamiyidans[1–4,56], the 'double engaged' occlusal pattern is clear: the distolabial main cusp A1 of M1 bites in the basin of m1, whereas the mesiolingual main cusp a1 of m1 occludes in the basin of M1. **f**, Computed laminography image showing the incisor germ within each jaw bone, located dorsal to the root of the enlarged incisor. a1l, Cusp a1 on left first lower molar; amf, anterior extremity of the masseteric fossa; b1l–b3l, Cusps b1, b2 and b3 on left first lower molar; dlp4, distal portion of left lower fourth premolar; lA1, A1 cusp of left first upper molar (it bites in the basin of m1); lA2, A2 cusp of left first upper molar (small cusp may exist between A1 and A2); ldI2, left second deciduous upper incisor; ldi, left deciduous lower incisor; ldii, left deciduous lower incisor impression; lig, left lower incisor tooth germ (successive incisor); lm1, left first lower molar; lM1, left first upper molar; lm2, left second lower molar; lM2, left second upper molar; lP3, left third upper premolar; lP4, left fourth upper premolar; mf, masseteric fossa; mlp4, mesial portion of left fourth lower premolar; plP4, partial left fourth upper premolar; rl2g, germ of right second upper incisor; rdI2, right second deciduous upper incisor; rdi, right deciduous lower incisor; rig, right lower incisor (successive) tooth germ; rldI2, root of second left upper deciduous incisor; rlM1, root of left first molar; rlP3, root of left their upper premolar; rm1, right first lower molar; rM1, right first upper molar; rm2, right second lower molar; rM2, right second upper molar; rP3, right third upper premolar; rp4, right fourth lower premolar; rP4, right fourth upper premolar; rrdi, root of right lower deciduous incisor; tldi, tip of left lower deciduous incisor.

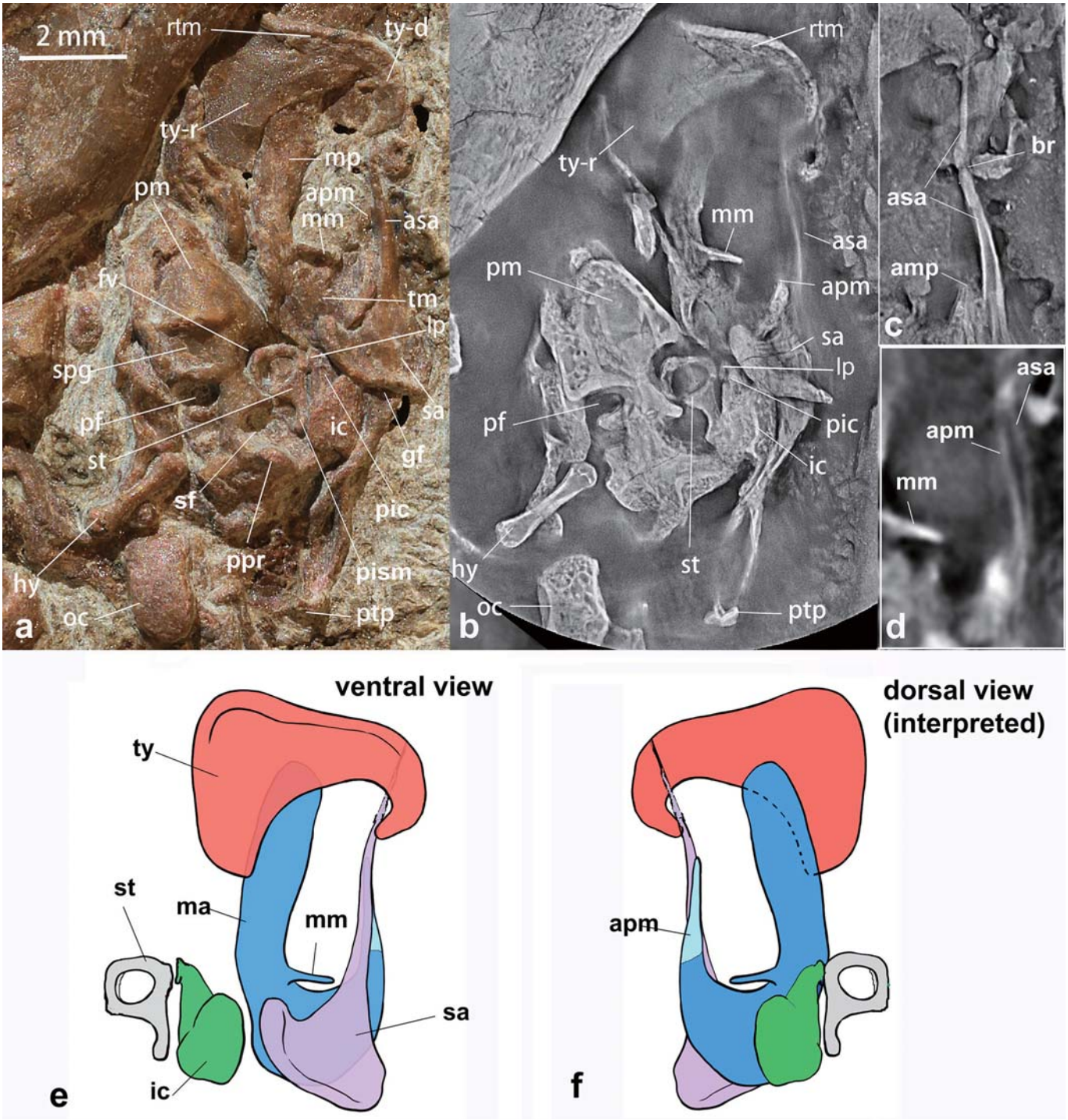

Extended Data Figure 5 | Auditory apparatus of *A. allinhopsoni* (holotype, HG-M017). **a**, Close-up view of the ear region (mostly left side) that corresponds to the boxed area in Fig. 2. **b**, Computed laminography image of the ear region. **c**, Computed laminography image showing the extension of the anterior process of the surangular. **d**, Computed laminography image showing the extension of the anterior process of the malleus. **e**, Interpretive drawing of the auditory bones (ventral view) with the stapes and incus moved out and the surangular overlapping with the malleus. **f**, Interpretative drawing of the auditory bones (dorsal view) with interpreted articulation of the incus and the malleus. Because the malleus, surangular and ectotympanic were slightly displaced from their anatomical positions, the reconstruction may not reflect the precise bone relationship. apm, anterior process of the malleus (prearticular); asa, anterior process of the surangular; br, breakage in the anterior process of the surangular; fv, fenestra vestibuli; gf, glenoid fossa; hy, hyoid element; ic, incus; lp, lenticular process; ma, malleus; mm, manubrium of the malleus; mp, medial process of the malleus; oc, occipital condyle; pf, perilymphatic foramen; pic, stapedial process of the incus; pism, process for insertion of the stapedius muscle of the stapes; pm, promontorium; ppr, paroccipital process; ptp, posttympanic process of the squamosal; rtm, ridge for attachment of the anterior part of the tympanic membrane; sa, surangular; sf, stapedius fossa; spg, groove for the stapedial artery; st, stapes; tm, transverse part of the malleus; ty, ectotympanic; ty-d, lateral ectotympanic part presumably equivalent to the dorsal part of the angular; ty-r, ectotympanic part presumably equivalent to the reflected lamina.

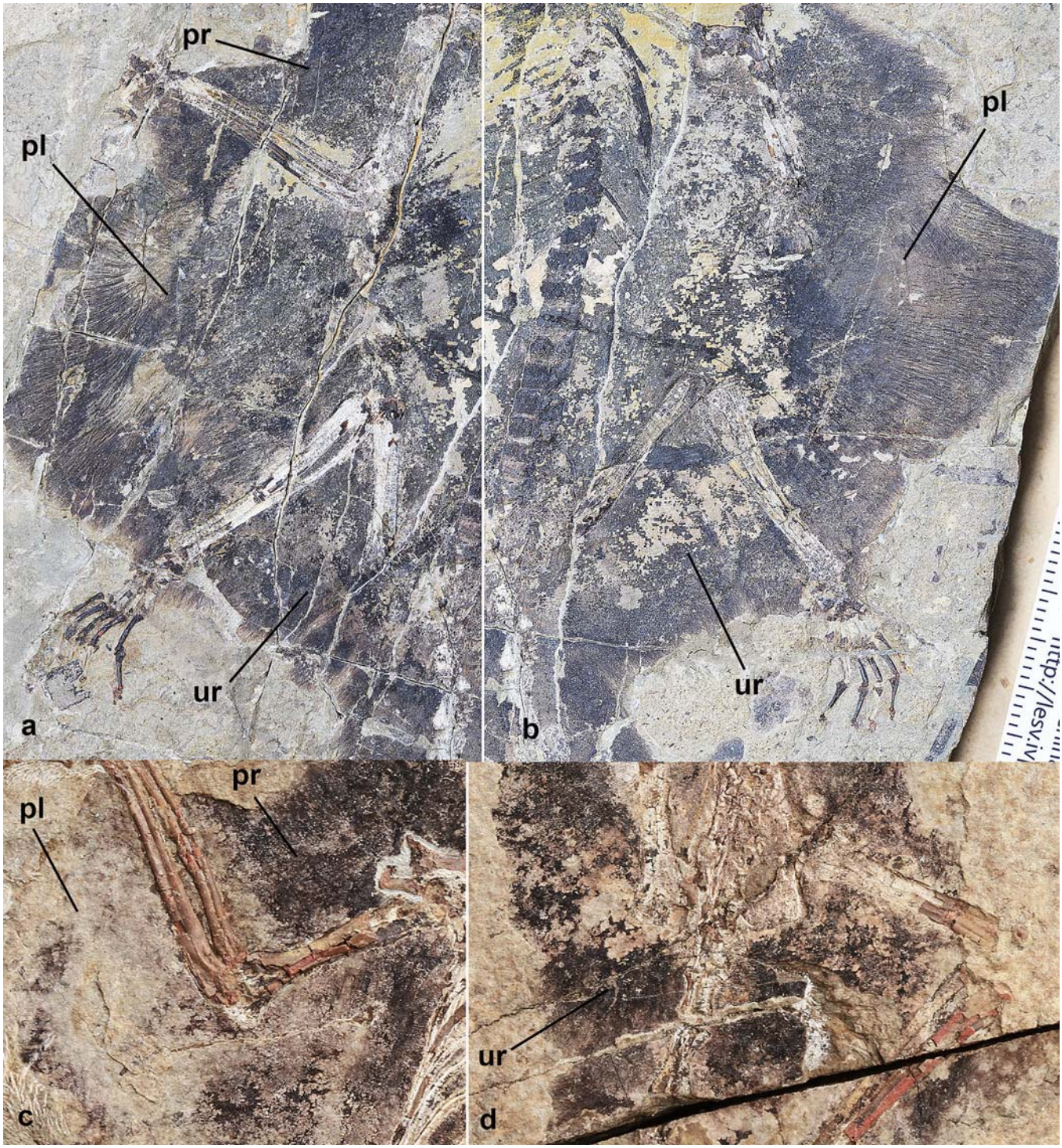

Extended Data Figure 6 | Limbs and gliding membrane of *A. allinhopsoni*. **a**, **b**, Close-up views showing the relationship of the limbs and the gliding membrane (paratype, HG-M018-A). Note that the forelimbs and hind limbs were flexed so that the gliding membrane is not preserved in its fully extended size. **c**, **d**, Close-up views showing the relationship of the limbs and the gliding membrane (holotype specimen, HG-M017). pl, plagiopatagium, the primary gliding membrane that extends between the forelimbs and hind limbs; pr, propatagium, the gliding membrane between the neck and forelimbs; ur, uropatagium, the gliding membrane between the hind legs and the tail.

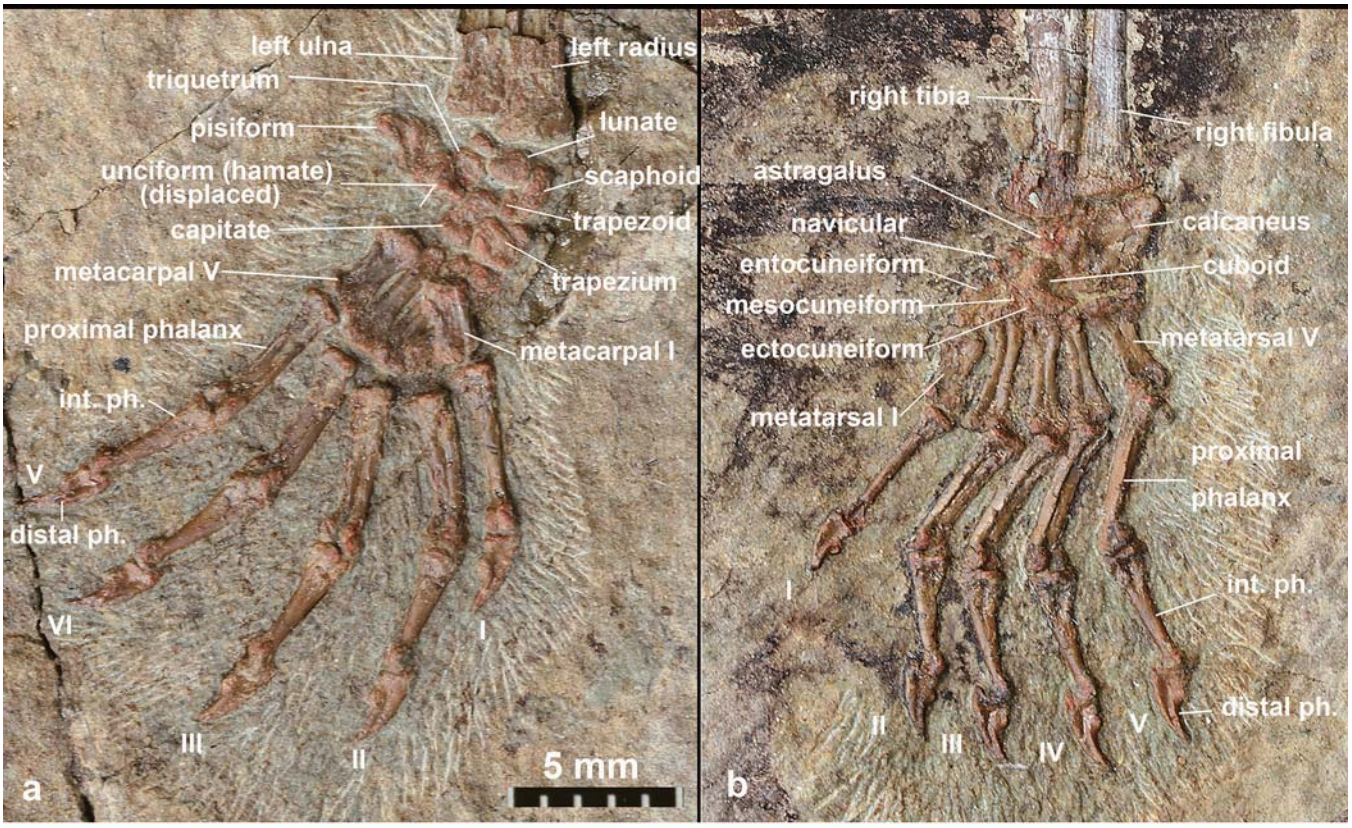

Extended Data Figure 7 | Manual and pedal structure and ternary diagrams showing the intrinsic ray III proportions. a, The manus in ventral view. **d**, The pes in ventral view. **a** and **b** are from the holotype, HG-M017-B. As in other euharamiyidans[1–4], the metapodials are short, whereas the phalanges are proportionally elongate. **c**, **d**, Ternary plots showing the relative lengths of the metapodial, proximal and intermediate phalanges for digit III of the manus and pes. The lengths of those elements are shown on their respective axes as a percentage of the combined length of the three segments. As in other euharamiyidans[8,9], *A. allinhopsoni* has a similar intrinsic manual and pedal ray proportion, which is typical of arboreal species in which the phalanges are long relative to the metapodials. In addition to the extant taxa, fossils involved in the plotting are: Ara, *A. allinhopsoni*; Arj, *A. jenkinsi*. Eo, *Eomaia scansoria*; Je, *Jeholodens jenkinsi*; Ma, *Maotherium sinensis*; Sb, *Sinobaatar lingyuanensis*; Sd, *Sinodelphys szalayi*; Sh, *Shenshou*; Xl, *X. linglong*; Xs, *Xianshou songae*. The plotting data are derived from previous studies[1,2].

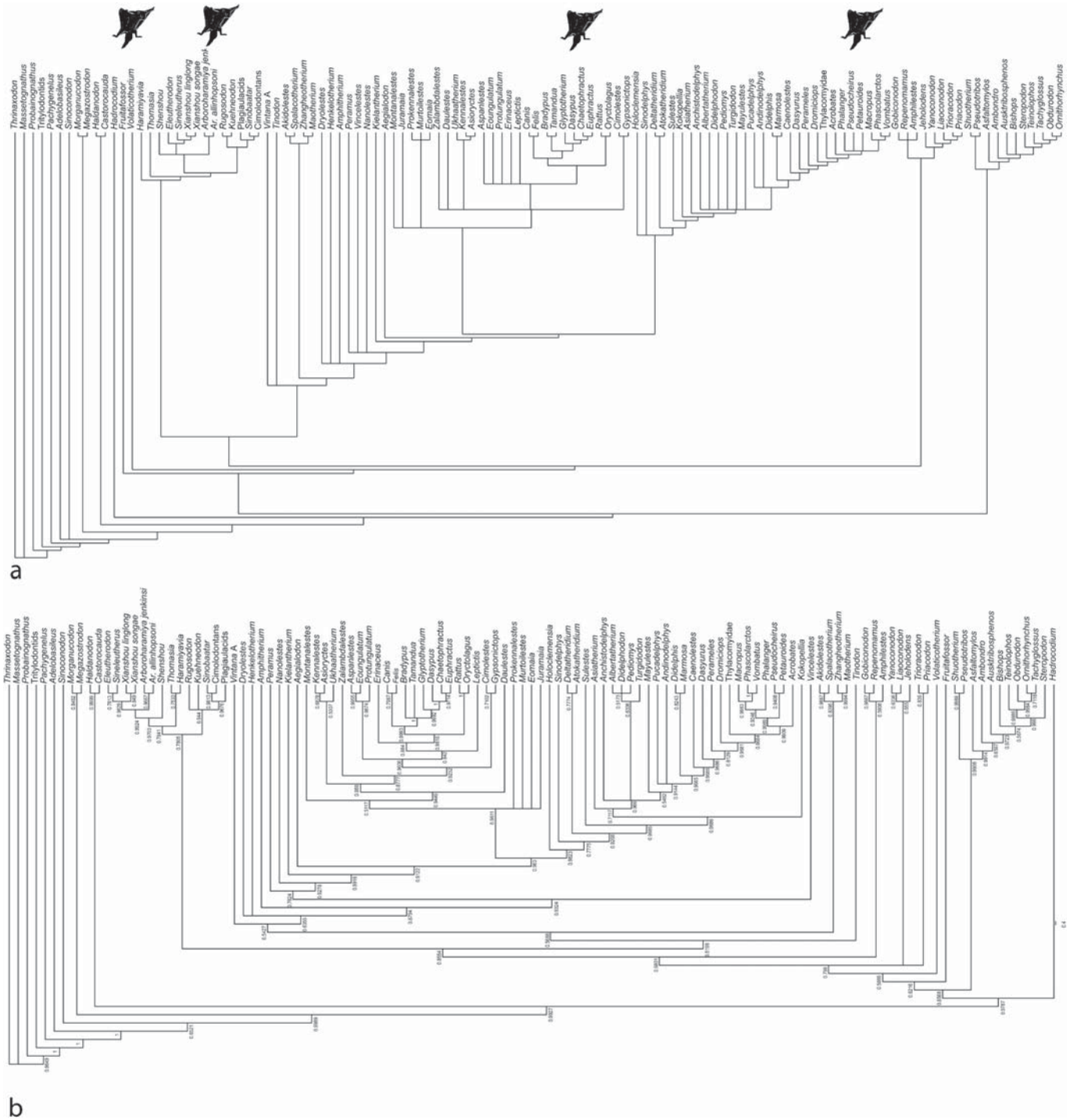

Extended Data Figure 8 | Results of phylogenetic analyses based on dataset I (*Vintana* A). a, Strict consensus tree resulted from parsimony-based analysis using PAUP*: tree length, 2,637; consistency index (CI), 0.3250; homoplasy index (HI), 0.6750; retention index (RI), 0.7895; rescaled consistency index (RC), 0.2566. **b**, Result of Bayesian analysis (50% majority-rule consensus) obtained from five million MCMC generations with burn-in fraction of 0.25. Node support given as posterior probabilities. See Methods and Supplementary Information for more details. In extant mammals, gliding locomotion has evolved independently in marsupials, rodents, and dermopterans[12,14], but they are not all illustratable.

Extended Data Table 1 | Measurements (in mm) of the type specimens of *A. allinhopsoni*

	Holotype (HG-M017)		Paratype (HG-M018)	
	Length	Width	Length	Width
Skull	30.8	?	27	19.9
Lower jaw	23.8			
Dentary	17.33			
R scapula	10.7	4.1		
L humerus	17.87	?	20	2.16
R humerus	17.82	1.95		
R ulna	22.58	1.7		
L ulna			24.5	1.5
R radius	19.65	1.73		
L radius			21.7	1.45
Metacarpal-proximal-intermediate-distal	I: 2.8-1.3-4.94-2.84 II: 4.1-4.96-4.15-3.3 III: 4.1-5.16-4.3-3.3 IV: 4.1-5.16-4.4-3.34 V: 3.25-4.8-4.25-3.1		I: 2.4-4.5-2.5 II: 2.8-4.6-4.1-2.5 III: 3.1-3.6*-?-? IV: 3.2-3.9*-4.25-2.55 V: 2.0-3.9-4.1-2.6	
R femur	21.0	2.7		
L femur			19.1	2.25
R tibias	21.5	2.1		
L tibias			24.7	1.8
R fibula	21.1	0.96		
L fibula			24	0.83
Metatarsal-proximal-intermediate-distal	I: 2.5-4.48-2.2 II: 3.9-4.8-3.8-2.3 III: 3.7-4.8-4.0-2.6 IV: 3.7-5.1-4.2-2.6 V: 3.2-5.1-4.2-2.7		I: 2.65-4.1-1.9 II: 3.2-4.4-3.57-2.7 III: 3.2-4.3-3.81-? IV: 3.6-4.3-3.95-2.5 V: 2.8-4.1-4.2-2.4	

R, right; L, left; asterisk indicates estimated measurement. *A. allinhopsoni* is smaller than *A. jenkinsi*. In terms of the mandible length (including the incisor), *A. allinhopsoni* is about 63% of *A. jenkinsi* (37.65 mm)[56]. In terms of the femur length, *A. allinhopsoni* is about 47% of *A. jenkinsi* (44.8 mm)[1].